IEEE Access
Multidisciplinary | Rapid Review | Open Access Journal

SPECIAL SECTION ON INTELLIGENT INFORMATION SERVICES

Received March 2, 2020, accepted March 24, 2020, date of publication April 3, 2020, date of current version April 20, 2020.

*Digital Object Identifier 10.1109/ACCESS.2020.2985527*

# New Results on Joint Classification of Vertical Structure of Ocean Properties at a Global Scale

**YANG FU[1,2,3], ZEYU ZHENG[1,2,3], MENGCHU ZHOU[4], (Fellow, IEEE), HAITAO YUAN[4], (Member, IEEE), AND XIWANG GUO[4,5]**

[1]Shenyang Institute of Automation, Chinese Academy of Sciences, Shenyang 110016, China
[2]Institutes for Robotics and Intelligent Manufacturing, Chinese Academy of Sciences, Shenyang 110016, China
[3]Key Laboratory of Network Control System, Chinese Academy of Sciences, Shenyang 110016, China
[4]Helen and John C. Hartmann Department of Electrical and Computer Engineering, New Jersey Institute of Technology, Newark, NJ 07102, USA
[5]Computer and Communication Engineering College, Liaoning Shihua University, Fushun 113001, China

Corresponding authors: Zeyu Zheng (zhengzeyu@sia.cn) and Mengchu Zhou (mengchu.zhou@njit.edu)

This work was supported in part by the Program for National Natural Science Foundation under Grant 71671182, in part by the Program for One-hundred Talent Program of the Chinese Academy of Sciences under Grant Y5AA100A01, in part by the Liaoning Revitalization Talents Program under Grant XLYC1907166, in part by the Liaoning Province Department of Education Foundation of China under Grant L2019027, and in part by the Liaoning Province Dr. Research Foundation of China under Grant 20170520135.

**ABSTRACT** Ocean temperature, salinity, and electric conductivity are essential ocean properties. Their structure and changes directly impact physical, chemical and biological processes in oceans. Since the 1970s, numerous researches have focused on the morphological analysis of vertical profiles in oceanography. However, due to the complexity of an ocean environment, most of them are conducted at local scales or only focus on single elements, e.g., ocean temperature or salinity. This work aims to achieve the joint classification of the vertical structure of ocean properties at a global scale and present two-dimension regional characteristics. Based on 150 seawater profiles from the National Oceanographic Data Center, this work explores such characteristics of ocean temperature, salinity and electric conductivity in the deep sea and achieves global-scale joint classification. We demonstrate that their vertical features have clear regional characteristics and can be classified into four types, i.e., bidirectional gradient, homo-dromous contravariant, homo-dromous gradient, and homodromous gradient (salinity) ones. In addition, our results prove that there exist the power-law distributions of these three factors in intermediate water, which may be explained through the self-organization theory. Moreover, the 'up-tail' phenomenon is widely discovered in the vertical structure of electric conductivity, and it may be considered as a combined effect caused by temperature, pressure, and salinity.

**INDEX TERMS** Vertical structure, joint classification, ocean temperature, salinity, electric conductivity, power-law behavior.

## I. INTRODUCTION

Ocean temperature, salinity, and electric conductivity are three critical oceanic environmental factors and can directly reflect the physicochemical, thermal, and electric properties of seawater [1], [2]. As they participate in the physical, chemical and biological processes of seawater, their structure and changes potentially affect marine dynamics, marine primary production, and the interactions between the marine system and climate changes [3]. Recent studies have particularly focused on the effect of these key processes, requiring accurate measurements of temperature, salinity, and conductivity to realize a deeper understanding of oceans and their interior [4], [5].

Numerous work has been conducted to analyze a vertical cross-section of oceanic factors at local scales [6]. The history can be traced back to the 1970s. For instance, Boguslavsky *et al.* (1994) carry out the numerical calculation of the vertical salinity profile in the Black Sea and analyzed its formation [7]. Gouskina *et al.* (1996) reveal the regular trend of three kinds of properties by investigating the spatial structure of the north pacific intermediate water [8]. In more

The associate editor coordinating the review of this manuscript and approving it for publication was Guanjun Liu.

recent efforts, Toyama and Suga (2010) examine the vertical structure of mode waters in the North Pacific by using Argo data and define the distribution area for each mode [9]. Damerell *et al*. (2016) present changes in the annual vertical structure of temperature, salinity, and oxygen concentration over 1000 meters of the ocean in the northeast Atlantic [10]. Yongcan, *et al*. (2019) explore the seasonal characteristics and the formation mechanism of the thermohaline structure of mesoscale eddy in the South China Sea and the results show that the vertical distribution of temperature exhibits a monolayer structure, while the salinity anomaly demonstrates a triple-layer structure [11]. However, due to the complexity of the marine environment, these studies reveal the substantial differences among them over various geographical regions [12]. For example, there are large differences in the spatial variability and the distribution of temperature and salinity in the North Atlantic and North Pacific regions [13]. The differences are mainly caused by submarine topography, local geographical and meteorological conditions, and ocean currents [14], [15]. Nevertheless, such metric analysis at local scales is unable to accurately account for the effect of oceanic factors to global material cycles and energy flow, and air-sea interaction. The reason is that the marine system is a complex dynamic structure where each component of the marine system affects each other [16], [17]. In addition, due to the remote sensing technology and the global profiling float program (Argo) that launched in the 2000s, it is easier to obtain the vertical structure characteristics of seawater properties on a global scale [18]. However, the deep-sea structural features are usually not observed and the resolution is relatively low.

Moreover, many sensitivity analyses of oceanic processes focus on one or two factors (e.g., sea temperature and thermohaline structure) rather than multiple ones [19]. For example, AquinoCruz and Aldo (2012) investigate the effect of seawater temperature on the growth and toxin production of three harmful benthic dinoflagellates and suggest that increasing seawater temperatures had a positive effect on them [20]. It is only a partial analysis to focus on a single factor in a marine system since ocean processes are better viewed as a combined interaction of various mutually dependent factors including ocean temperature, seawater chemistry and marine organism [21], [22]. As shown in various findings, some oceanic factors are highly related to each other [23]. For instance, it has been demonstrated that the electrical conductivity of seawater is associated with salinity, temperature, and pressure [24]. This association among oceanic factors strengthens the role of oceanic processes [25]. Hence, an exhibition of the global pattern on comprehensive factors can help us further understand the comprehensive effect of oceanic factors on various processes of ocean and predictive abilities regarding changes in a marine environment.

This work adopts the CTD (conductivity-temperature-depth) profiles provided by the National Oceanographic Data Center (NODC), which widely distributed on a global basis. The contribution of it are: (1) It makes a global-scale joint classification of vertical structure characteristics of ocean properties for the first time. The results show that their vertical features have clear regional characteristics and can be classified into four types. (2) It reveals the power-law distributions of these three factors in intermediate water. And (3) It explains the 'up-tail' phenomenon widely found in the conductivity vertical structure, considered as a combined effect of temperature, pressure, and salinity.

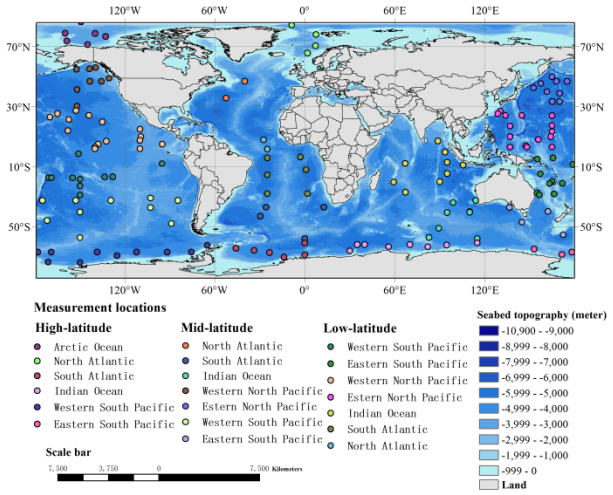


**FIGURE 1. Geographic locations of 150 CTD profiles. The map was created by ArcMap 9.3 [40].**

## II. DATA AND METHODS

The CTD profiles for this investigation are obtained from the World Ocean Database 2013 (WOD13), provided by NODC. It has been widely adopted for oceanographic, climate, and modeling researches [26], [27]. In this work, the CTD profiles are selected in the WOD select mode and sorted by ocean area and latitudes (Fig. 1). This work prefers to choose the profiles whose maximum measured depth is below 3000 meters and they are distributed throughout the global oceans. We screen and finally chose 150 CTD profiles to conduct our research. The records of temperature and salinity spanned the period from 1981 to 2016. In temperate regions, about half of the CTD profiles are produced in summer. It is also worth noting that there is no electric conductivity data in the WOD13 data set. So conductivity is calculated from salinity, temperature, and pressure with the Practical Salinity Scale 1978 [28], [29].

We complete the classification work in four steps, as follows:

Step 1. Data pre-processing.

Due to inconsistent records of the raw data, we make the process of data pretreatment. Firstly, these records are usually binned in a depth of 1 to 5 meters, and some are calculated by using smaller-depth intervals. Therefore, we unify all these CTD records to a 5 m-depth interval. Secondly, we remove the redundant data, which are caused by the fluctuating movement of the ships in the shallow water. Lastly, we wipe off the abnormal data. Since individual data may be impractical or lost due to environmental interference or human

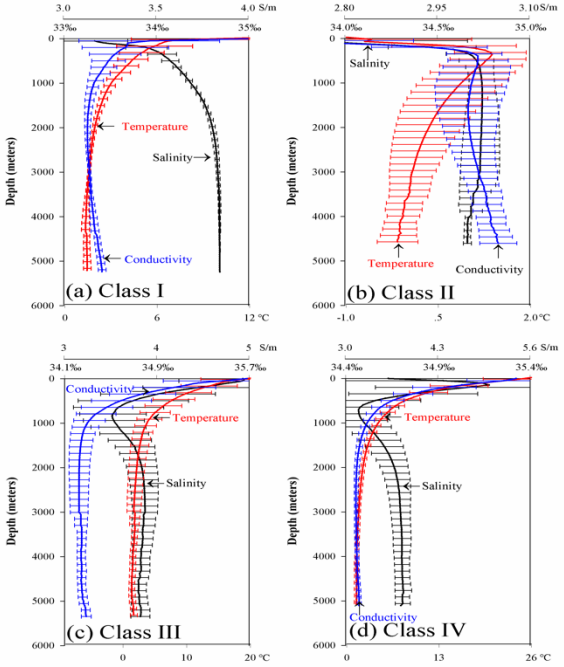


**FIGURE 2.** The vertical structures of temperature, salinity and electric conductivity with standard deviations, and indicative of the tightness of each curve.

factors during the collection and transmission of measurement data.

Step 2. Determination of the typical vertical structure for three ocean factors.

Existing literature shows that there are local variations in salinity and temperature in the distinct geographic locations. For example, previous research has reported decreases in Atlantic Ocean water salinity with depth, which is the opposite of the observed trend in the Pacific. By investigating existing materials and data, we determine the typical vertical structure for three ocean factors, including two types of temperature, three types of salinity and two types of conductivity. Then, we select them as the reference structures for the subsequent similarity calculation.

Step 3. Shape similarity measurement based on the DTW algorithm.

The dynamic time warping (DTW) algorithm is used to measure the similarity between the target data and the template data (reference structures). Its principle is to build an adjacency matrix of two series and find a path along which the cumulative distortion between the two series is minimized [30]–[32].

We set two series $P = (p_1, p_2, p_3, \ldots p_m)$ and $Q = (q_1, q_2, q_3, \ldots q_n)$. The adjacency matrix of two series is defined as $D_{n\times m} = \{dist(i,j)\}_{n\times m}$ where $dist(i,j) = (p_i - q_j)^2$. The path is optimized by the dynamic programming technique [33], [34], and can be expressed as below:

$$DTW(i,j) = dist(p_i, q_j) + \min \begin{cases} DTW(i, j-1) \\ DTW(i-1, j-1) \\ DTW(i-1, j) \end{cases} \quad (1)$$

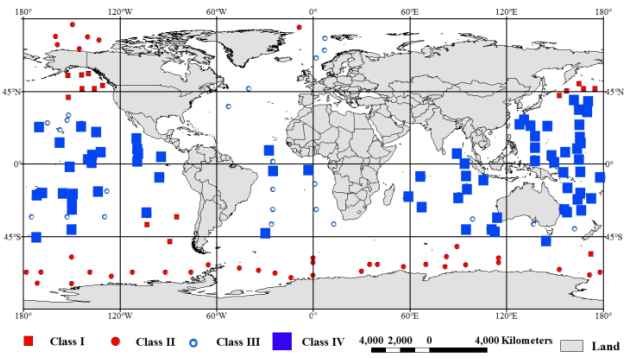


**FIGURE 3.** The distribution map of four types of temperature, salinity, and electric conductivity. The map was created by ArcMap 9.3 [40].

where $p_i$ and $q_j$ are the $i$th and $j$th values of series $P$ and $Q$.

The DTW alignment distance between the target data and the template data is taken as the feature factor of the next comprehensive classification [35], [36].

Step 4. Comprehensive classification based on three factors.

In this step, we compare the DTW distance between each type of ocean factor in the target data and the reference structure and choose the typical structure with the nearest distance as its ownership structure [37]–[39]. After classifying the structural types of the three ocean factors, the factors comprehensive taxonomy is used to make the comprehensive classification process for the 150 CTD profiles. The structural types of salinity, temperature, and conductivity are taken as the classification elements. Those CTD profiles in which the structural types of three elements are the same are classified into one class.

After the above procedures, we calculate the mean and standard deviation of ocean temperature, salinity and electric conductivity for each class to reveal the vertical structure.

## III. RESULTS

### A. FOUR CLASSES OF OCEANIC FACTOR VERTICAL STRUCTURES

Based on vertical profiles of temperature, salinity, and electric conductivity, their vertical structures can be divided into four classes: bidirectional gradient, homodromous contravariant, homodromous gradient, and homodromous gradient (salinity) ones as shown in Figs. 2 and 3.

*Class I. 'Bidirectional Gradient' Type:*

Temperature and conductivity decrease rapidly from sea surface to about 500 m depth. With the increase of depth, temperature and conductivity reach a minimum at about 3000 m and 2000 m, respectively. The minimums are separately referred to as the temperature minimum ($T_{min}$) and conductivity minimum ($C_{min}$) layer. Below the $T_{min}$ and $C_{min}$ layer, temperature and conductivity slowly increase toward the bottom, where the temperature increases in abyssal region due to adiabatic compression. In contrast, salinity reaches its maximum at about 3000 m depth, and then it preserves its

value from 3000 m to the bottom. Observation sites in this category are mainly distributed in high and middle latitudes of North Pacific (40–60°N and 35–55°S).

*Class II. 'Homodromous Contravariant' Type:*

Salinity, temperature, and conductivity increase rapidly to their maximum from sea surface to subsurface. Their maximums are separately referred to as the salinity maximum ($S_{max}$), temperature maximum ($T_{max}$), and conductivity maximum ($C_{max}$) layer. Below these maximum layers, salinity and temperature decrease monotonously down to the bottom. Conductivity below its maxima at about 300 m decreases in deeper layers. There is a salinity minimum at about 2300 m depth, referred to as the conductivity minimum ($C_{min}$) layer. From the $C_{min}$ layer to the bottom, conductivity slowly increases in the deep ocean. Observation sites in this category are mainly distributed in the Antarctic and the Arctic Ocean.

*Class III. 'Homodromous Gradient' Type:*

Salinity, temperature, and conductivity decrease rapidly from sea surface to about 1000 m depth. With the increase of depth, temperature and conductivity reach their minimum at about 4000 m and 3000 m, respectively. Their minimums are separately referred to as the temperature minimum ($T_{min}$) and conductivity minimum ($C_{min}$) layer. Below the $T_{min}$ and $C_{min}$ layer, temperature and conductivity slowly increase toward the bottom. From 1000 m to 3500 m depth, salinity increases. Below 3500 m depth in the bottom direction, salinity preserves the same value. Observation sites in this category are mainly distributed at low and middle latitudes of the west Pacific Ocean and the Atlantic Ocean. In addition, three sites are found at high latitudes of the Atlantic Ocean and the other three are found at low latitudes of the southern Indian Ocean and Southeast Pacific Ocean.

*Class IV. 'Homodromous Gradient (Salinity)' Type:*

The vertical structure in this category is similar to the 'homodromous gradient' type but it contains two haloclines in the vertical structure of salinity. Temperature and conductivity decrease rapidly from sea surface to about 1000 m depth. With the increase of depth, temperature and conductivity reach the minimum at about 4000 m and 3000 m, respectively. Again, below the depth where the minimum is achieved, temperature and conductivity slowly increase toward the bottom. The salinity increases rapidly to the maximum value from the sea surface to subsurface. It is referred to as the salinity maximum ($S_{max}$) layer. From the $S_{min}$ layer that is recorded at about 800 m depth, salinity decreases rapidly to its minimum, which referred to as the salinity minimum ($S_{min}$) layer. From the $S_{min}$ layer to 3000 m depth, salinity increases again. Below 3000 m depth downwards, salinity keeps its constant value. Observation sites in this category are mainly distributed in the eastern Pacific Ocean and the Indian Ocean. A few observation sites are in the tropical and subtropical regions of the west Pacific Ocean and the Atlantic Ocean.

### B. POWER-LAW BEHAVIORS IN INTERMEDIATE WATER

The relations between depth and oceanic factors are presented on a log-log plot in Fig. 4, and some show a linear relation

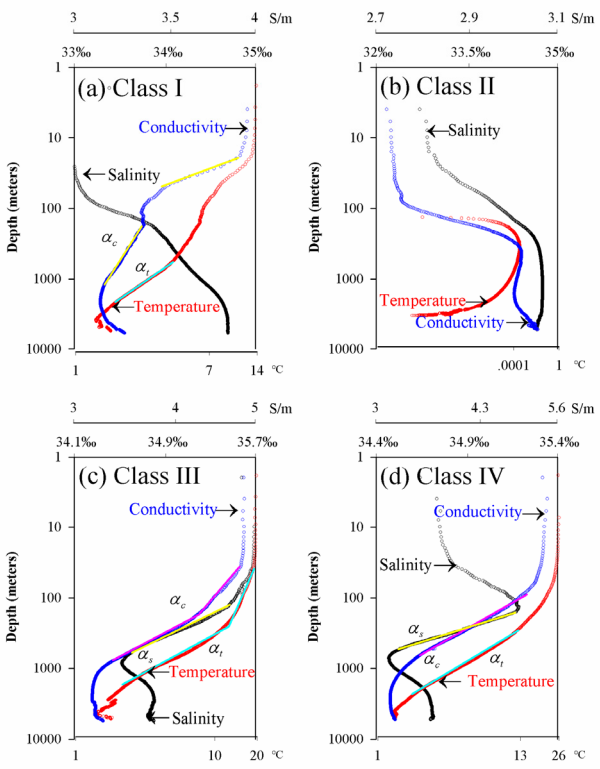


**FIGURE 4.** Log–Log plot of the vertical structure of temperature, salinity, and electric conductivity.

at the subsurface and intermediate layer, which can be well described by a power-law distribution, i.e.,

$$F(d) \sim d^{-\alpha} \tag{2}$$

where $F(d)$ is an oceanic factor, $d$ is sea depth, and $\alpha$ is a power exponent. Usually, the value of $\alpha$ is greater than zero.

In Fig. 4, $\alpha_t$ is the power exponent of temperature $T$, $\alpha_s$ is the power exponent of salinity, and $\alpha_c$ is the power exponent of conductivity. They are indicated by three-line segments in cyan, yellow and pink, respectively. The $R^2$ values are the coefficients of determination for the fitting line segments on the log-log plots. All $R^2$ values for line segments are greater than 0.99.

Besides Class II, the power-law behaviors always exist in the vertical structure of temperature, salinity, and conductivity at middle-low latitudes. It is observed that multiple power-law behaviors may occur in one CTD profile (e.g., Fig. 4c). Moreover, there remain some differences among temperature, salinity, and conductivity shown in Table 1. All power-law exponents of temperature exhibit the maximal value, wherein we find that a vase of salinity is the minimum. The power-law exponent of conductivity is generally less than 0.2. For the depth range, the power-law behavior existing in the vertical structure of temperature is wide and the maximum value is reached at 3000 m depth. For temperature, the power-law behavior occurs approximately between 100 and 700 m depth. The power-law behavior in the vertical structure of

**TABLE 1. Description of the power-law behaviors that exist in the vertical structure of temperature (T), salinity (S), and conductivity (C).**

| | | Class I | Class II | Class III | Class IV |
|---|---|---|---|---|---|
| *T* | $-\alpha_t$ | -0.6235 | - | -0.2113, -0.9008 | -0.9201 |
| | Depth | 532~2973 | - | 36~208, 208~2002 | 230~2603 |
| | $R^2$ | 0.999 | - | 0.991, 0.992 | 0.997 |
| *S* | $-\alpha_s$ | - | - | -0.0171 | -0.0147 |
| | Depth | - | - | 127~622 | 151~678 |
| | $R^2$ | - | - | 0.998 | 0.994 |
| *C* | $-\alpha_c$ | -0.1241, -0.0324 | - | -0.0809, -0.1572 | -0.1839 |
| | Depth | 18~52, 165~1220 | - | 36~195, 195~1188 | 66~790 |
| | $R^2$ | 0.992, 0.997 | - | 0.995, 0.995 | 0.997 |

conductivity occurs for a depth range approximately between several tens to about 1000 m.

## IV. DISCUSSION

In this work, we offer a joint study on ocean temperature, salinity, and electric conductivity and classify them into four major types on a global scale. The temperature and salinity are two important parameters of marine hydrology and have been widely adopted to analyze hydrographic features and water masses. They interact with each other and act on multiple processes at the same time. Numerous researches use the TS-diagram to explore their characteristics, while we study the dynamic evolution mode of them by using the space panel data analysis method. Additionally, we encompass conductivity into classification, since ocean conductivity is a fundamental parameter in electromagnetic reflection, which has a great influence on the process of marine biological and physical processes. For instance, Irrgang *et al*. (2015) find that the temporal variability of the magnetic field increase by 45% through the use of the true global conductivity distribution of seawater [41], [42].

Our results accord with earlier observations [43]. In low latitudes, we define the type as 'homodromous gradient', characterized by a vertical structure that first decreases with depth and then slowly increases below some specific depth. This finding corresponds to previous studies and is usually found in the Atlantic, Pacific and tropical oceans [44]. Furthermore, we define the 'homodromous gradient (salinity)' type, mainly because salinity has a rapid increase (represented as a small spike in Fig. 2(d) in the subsurface layer of the ocean. Current work has attributed the small spike to the high salt content water which sinks at the northern and southern middle latitudes and extends to the equator [45]. For the middle and high latitudes, we define the 'bidirectional gradient' (distributed in high and middle latitudes of North Pacific) and the 'homodromous contravariant' type (distributed in the Antarctic and Arctic Ocean), respectively, according to the vertical features of these three factors. The difference between them is whether the change in the trend of salinity is consistent with those of the other two factors. The results indicate that sea salinity, temperature, and conductivity increase rapidly to their maximum from sea surface to the subsurface in polar regions, largely due to the cold climate [46]. In the regions of 40–60°N and 35–55°S, we find that salinity increases with depth while temperature and conductivity decrease from sea surface to about 2000 m depth. The observation is consistent with previous studies and it is attributed to a combined effect of the freshwater exchange across the air-sea boundary, the northward transport of water, heat transfer at the air-sea boundary and vertical mixing [47].

In addition, the 'up-tail' phenomenon is widely found in the vertical structures of temperature (except for Class II) and conductivity (in all four classes). The warped-tail phenomenon of temperature is previously revealed and attributed their formation to the adiabatic heating [48]. However, the warped-tail phenomenon for conductivity is often neglected [49]. To account for this, there are three factors for driving the slow rise of conductivity in deep sea. The first reason is high salinity. It increases the ionic concentration in seawater [50], [51]. The second reason is increasing temperature. It can positively affect conductivity [52]. The third reason is high seawater pressure, which leads to an increase in the ionic concentration in seawater [53], [54]. Our results indicate that increasing conductivity in deep oceans can be regarded as a combined effect of temperature, pressure, and salinity. Increasing salinity and pressure can positively affect conductivity while decreasing temperature leads to a negative effect [55]. However, more controlled experiments are required in future research to quantify the effect of each factor on seawater conductivity [56].

Moreover, it is worth noting that conductivity varies consistently with temperature from sea surface to about 2000 m depth. In abyssal region, the difference in the changing trend of conductivity and temperature increases gradually. For salinity, it is considered that conductivity and salinity are in the direct ratio [57]. However, the variation tendency between conductivity and salinity are opposites in Class I, as observed in high and middle latitudes of North Pacific. Several reports have suggested that salinity is the main factor for conductivity [55]. However, our findings suggest that temperature has a greater influence on the vertical structure of conductivity above abyssal region. Correlation analysis between conductivity and temperature has also been conducted, and the results indicate that conductivity has a high linear relationship with temperature from the sea surface to 2000 m depth, with $R^2 = 0.99$ [58].

Furthermore, we observe that power-law behaviors could govern the statistics of three oceanic factors in intermediate

water at middle-low latitudes. The power function model with the decay coefficient (except for salinity in Class I and temperature, salinity, and conductivity in Class II) is constructed to describe the vertical structures of oceanic factors and to reveal the inherent dynamic mechanism. Based on this observation, we put forward the hypothesis that the change of vertical structure is a self-organized critical process. This argument suggests that the vertical change of oceanic factors follows a dynamical adapting mechanism in a certain depth range, *i.e.*, an intermediate water layer automatically evolves towards an equilibrium state, and the process is spontaneous. We believe that the ocean is an open dissipative system at middle-low latitudes and meets the following conditions for its formation.

Firstly, the ocean is constantly exchanging material and energy with the external environment (such as the atmosphere), and therefore the system is open [59].

Secondly, there are complex coupling effects of mechanics, thermology, electricity, magnetism, and hydrochemistry among the marine internal subsystems, and therefore the input-output relationship of the system does not satisfy the homogeneity and superposition [60]. It means that the system has a nonlinear interaction.

Thirdly, the ocean system is a part of the earth's evolution, which is spatio-temporal symmetry-breaking and far away from the equilibrium state. Moreover, the system is subject to the combined action of the external loading and environmental factors (such as the tidal stress and the rotation of the earth), and therefore the system is non-equilibrium [61], [62].

Lastly, the ocean is composed of many water masses (subsystems), and each subsystem can be regarded as a thermodynamic system. Thus, the ocean system satisfies the partial thermal equilibrium assumption [63].

To sum up, it is appropriate to analyze the ocean's spatiotemporal property with the self-organization theory. Due to the complex interaction among the subsystems in the ocean system and the complex constraint relationship between the system and the external environment, its spatiotemporal property shows a kind of mutual system and overall evolution behavior. Therefore, the power-law behavior of ocean factors is a kind of a spatial structure obtained by the internal self-organization of the ocean system at middle-low latitudes, which embodies its scale invariance in space. Furthermore, the power-law distribution of sea temperature can be regarded as a dissipative structure in thermodynamics, and the power-law distribution of salinity can also be regarded as a Belousov-Zhabotinskii (B-Z) oscillating reaction. The power-law distribution of electrical conductivity can be regarded as the scale-invariant structure of ocean electromagnetic characteristics. The new insights into the vertical structure feature formation should greatly contribute to exploring the dynamic properties of seawater.

Many studies refer to the oceanic mixed layer, characterized by a nearly homogeneous distribution of properties [64], [65]. It seems that such a mixed layer is not present in our results (Fig. 2), because most of the measurements we chose are collected during the summer when the depth of a mixing layer is very small [66], [67]. It has been demonstrated that the depth of the mixed layer is greater in winter than that in summer in each hemisphere. The reason for this is that solar heating of the surface water increases in summer, which makes the density stratification more stable and reduces the penetration of wind-driven mixing [68], [69]. Hence, a mixed layer is not easy to distinguish with our naked eye in Fig. 2. Nevertheless, a mixed layer is shown to exist in Fig. 3, which can be approximated by a constant reflected on a double logarithmic axis. We find that the vertical structure of conductivity is nearly uniform in the mixed layer.

## V. CONCLUSION

This work performs a global-scale joint classification of the vertical structure of ocean temperature, salinity, and electric conductivity and presents the regional characteristics. The results reveal that these three factors can be classified into four classes and there exist the power-law distributions of them in intermediate water. We explain it through the self-organization theory. In addition, we find that the 'up-tail' phenomenon is widely discovered in the vertical structure of electric conductivity, and attribute it to a combined effect caused by temperature, pressure, and salinity. This work provides a reference value for the comprehensive effect of oceanic factors on a variety of ocean processes. Some recent neural network methods, e.g., [70], can be used to refine the classification work presented in this paper, thereby gaining more insight into ocean properties at regional/local levels.

## REFERENCES

[1] T. Lee, S. Fournier, A. L. Gordon, and J. Sprintall, "Maritime continent water cycle regulates low-latitude chokepoint of global ocean circulation," *Nature Commun.*, vol. 10, no. 1, pp. 1–13, Dec. 2019.

[2] S. L. Neal, R. L. Mackie, J. C. Larsen, and A. Schultz, "Variations in the electrical conductivity of the upper mantle beneath north america and the pacific ocean," *J. Geophys. Res., Solid Earth*, vol. 105, no. B4, pp. 8229–8242, Apr. 2000.

[3] R. Pawlowicz, D. G. Wright, and F. J. Millero, "The effects of biogeochemical processes on oceanic conductivity/salinity/density relationships and the characterization of real seawater," *Ocean Sci.*, vol. 7, no. 3, pp. 363–387, 2011.

[4] L. Wang, Y. Wang, J. Wang, and F. Li, "A high spatial resolution FBG sensor array for measuring ocean temperature and depth," *Photon. Sensors*, vol. 10, no. 1, pp. 57–66, Mar. 2020.

[5] J. Etourneau, G. Sgubin, X. Crosta, D. Swingedouw, V. Willmott, L. Barbara, M.-N. Houssais, S. Schouten, J. S. S. Damsté, H. Goosse, C. Escutia, J. Crespin, G. Massé, and J.-H. Kim, "Ocean temperature impact on ice shelf extent in the eastern antarctic peninsula," *Nature Commun.*, vol. 10, no. 1, pp. 1–8, Dec. 2019.

[6] B. B. Nardelli and R. Santoleri, "Methods for the reconstruction of vertical profiles from surface data: Multivariate analyses, residual GEM, and variable temporal signals in the north pacific ocean," *J. Atmos. Ocean. Technol.*, vol. 22, no. 11, pp. 1762–1781, Nov. 2005.

[7] S. G. Boguslavsky, V. A. Zhorov, and I. K. Ivashchenko, "Formation of the vertical salinity profile in the black sea," *Phys. Oceanogr.*, vol. 5, no. 6, pp. 443–449, Nov. 1994.

[8] W. Zenk, G. Siedler, A. Ishida, J. Holfort, Y. Kashino, Y. Kuroda, T. Miyama, and T. J. Müller, "Pathways and variability of the antarctic intermediate water in the western equatorial pacific ocean," *Prog. Oceanogr.*, vol. 67, nos. 1–2, pp. 245–281, Oct. 2005.

[9] K. Toyama and T. Suga, "Vertical structure of north pacific mode waters," *Deep Sea Res. II, Topical Stud. Oceanogr.*, vol. 57, nos. 13–14, pp. 1152–1160, Jul. 2010.
[10] G. M. Damerell, K. J. Heywood, A. F. Thompson, U. Binetti, and J. Kaiser, "The vertical structure of upper ocean variability at the porcupine abyssal plain during 2012–2013," *J. Geophys. Res., Oceans*, vol. 121, no. 5, pp. 3075–3089, May 2016.
[11] Y. Zu, S. Sun, W. Zhao, P. Li, B. Liu, Y. Fang, and A. A. Samah, "Seasonal characteristics and formation mechanism of the thermohaline structure of mesoscale eddy in the South China Sea," *Acta Oceanol. Sinica*, vol. 38, no. 4, pp. 29–38, Apr. 2019.
[12] M. D. Skogen, A. Olsen, K. Y. Børsheim, A. B. Sandø, and I. Skjelvan, "Modelling ocean acidification in the nordic and barents seas in present and future climate," *J. Mar. Syst.*, vol. 131, pp. 10–20, Mar. 2014.
[13] N. J. Delorme and M. A. Sewell, "Temperature and salinity: Two climate change stressors affecting early development of the New Zealand sea urchin Evechinus chloroticus," *Mar. Biol.*, vol. 161, no. 9, pp. 1999–2009, Sep. 2014.
[14] C. Wang and L. Zhang, "Multidecadal ocean temperature and salinity variability in the tropical North Atlantic: Linking with the AMO, AMOC, and subtropical cell," *J. Climate*, vol. 26, no. 16, pp. 6137–6162, Aug. 2013.
[15] W. S. Broecker, "The salinity contrast between the Atlantic and pacific oceans during glacial time," *Paleoceanography*, vol. 4, no. 2, pp. 207–212, Apr. 1989.
[16] Y. Plancherel, "Hydrographic biases in global coupled climate models and their relation to the meridional overturning circulation," *Climate Dyn.*, vol. 44, nos. 1–2, pp. 1–44, Jan. 2015.
[17] M. F. de Jong, S. S. Drijfhout, W. Hazeleger, H. M. van Aken, and C. A. Severijns, "Simulations of hydrographic properties in the northwestern North Atlantic Ocean in coupled climate models," *J. Climate*, vol. 22, no. 7, pp. 1767–1786, Apr. 2009.
[18] C. Cabanes, V. Thierry, and C. Lagadec, "Improvement of bias detection in argo float conductivity sensors and its application in the North Atlantic," *Deep Sea Res. I, Oceanogr. Res. Papers*, vol. 114, pp. 128–136, Aug. 2016.
[19] C. Stegert, R. Ji, and C. S. Davis, "Influence of projected ocean warming on population growth potential in two North Atlantic copepod species," *Prog. Oceanogr.*, vol. 87, nos. 1–4, pp. 264–276, Oct. 2010.
[20] E. Cortijo, S. Lehman, L. Keigwin, M. Chapman, D. Paillard, and L. Labeyrie, "Changes in meridional temperature and salinity gradients in the North Atlantic Ocean (30°-72°N) during the last interglacial period," *Paleoceanography*, vol. 14, no. 1, pp. 23–33, Feb. 1999.
[21] M. Ikeda, "Salt and heat balances in the Labrador sea using a box model," *Atmos.-Ocean*, vol. 25, no. 2, pp. 197–223, Jun. 1987.
[22] A. Mariotti, "Recent changes in the mediterranean water cycle: A pathway toward long-term regional hydroclimatic change?" *J. Climate*, vol. 23, no. 6, pp. 1513–1525, Mar. 2010.
[23] R. W. Schmitt, "Form of the temperature-salinity relationship in the central water: Evidence for double-diffusive mixing," *J. Phys. Oceanogr.*, vol. 11, no. 7, pp. 1015–1026, Jul. 1981.
[24] R. Pawlowicz, "The electrical conductivity of seawater at high temperatures and salinities," *Desalination*, vol. 300, pp. 32–39, Aug. 2012.
[25] S. D. Kashenko, "The combined effect of temperature and salinity on development of the sea star Asterina pectinifera," *Russian J. Mar. Biol.*, vol. 32, no. 1, pp. 37–44, Mar. 2006.
[26] A. Johari and M. F. Akhir, "Exploring thermocline and water masses variability in southern South China Sea from the world ocean database (WOD)," *Acta Oceanol. Sinica*, vol. 38, no. 1, pp. 38–47, Jan. 2019.
[27] R. Showstack, "World ocean database," *Eos, Trans. Amer. Geophys. Union*, vol. 90, no. 49, p. 472, 2009.
[28] E. Lewis, "The practical salinity scale 1978 and its antecedents," *IEEE J. Ocean. Eng.*, vol. OE-5, no. 1, pp. 3–8, Jan. 1980.
[29] E. L. Lewis and R. G. Perkin, "The practical salinity scale 1978: Conversion of existing data," *Deep Sea Res. A. Oceanograph. Res. Papers*, vol. 28, no. 4, pp. 307–328, Apr. 1981.
[30] R. J. Kate, "Using dynamic time warping distances as features for improved time series classification," *Data Mining Knowl. Discovery*, vol. 30, no. 2, pp. 283–312, Mar. 2016.
[31] G. Forestier, F. Lalys, L. Riffaud, B. Trelhu, and P. Jannin, "Classification of surgical processes using dynamic time warping," *J. Biomed. Informat.*, vol. 45, no. 2, pp. 255–264, Apr. 2012.
[32] D. Folgado, M. Barandas, R. Matias, R. Martins, M. Carvalho, and H. Gamboa, "Time alignment measurement for time series," *Pattern Recognit.*, vol. 81, pp. 268–279, Sep. 2018.
[33] H. Yuan, J. Bi, B. H. Li, and W. Tan, "Cost-aware request routing in multi-geography cloud data centres using software-defined networking," *Enterprise Inf. Syst.*, vol. 11, no. 3, pp. 359–388, Mar. 2017.
[34] H. Yuan, J. Bi, W. Tan, and B. H. Li, "CAWSAC: Cost-aware workload scheduling and admission control for distributed cloud data centers," *IEEE Trans. Autom. Sci. Eng.*, vol. 13, no. 2, pp. 976–985, Apr. 2016.
[35] J. Bi, H. Yuan, and M. Zhou, "Temporal prediction of multiapplication consolidated workloads in distributed clouds," *IEEE Trans. Autom. Sci. Eng.*, vol. 16, no. 4, pp. 1763–1773, Oct. 2019.
[36] J. Bi, H. Yuan, L. Zhang, and J. Zhang, "SGW-SCN: An integrated machine learning approach for workload forecasting in geo-distributed cloud data centers," *Inf. Sci.*, vol. 481, pp. 57–68, May 2019.
[37] H. Darabi, G. Ifrim, P. Schafer, and D. F. Silva, "Guest editorial for special issue on time series classification," *IEEE/CAA J. Autom. Sinica*, vol. 6, no. 6, pp. 1291–1292, Nov. 2019.
[38] T. Lintonen and T. Raty, "Self-learning of multivariate time series using perceptually important points," *IEEE/CAA J. Autom. Sinica*, vol. 6, no. 6, pp. 1293–1305, Nov. 2019.
[39] H. A. Dau, A. Bagnall, K. Kamgar, C.-C.-M. Yeh, Y. Zhu, S. Gharghabi, C. A. Ratanamahatana, and E. Keogh, "The UCR time series archive," *IEEE/CAA J. Autom. Sinica*, vol. 6, no. 6, pp. 1293–1305, Nov. 2019.
[40] T. Ormsby, E. Napoleon, R. Burke, and C. Groessl, *Getting to Know ArcGIS Desktop*. Redlands, CA, USA: ESRI Press, 2001.
[41] C. Irrgang, J. Saynisch, and M. Thomas, "Impact of variable sea-water conductivity on motional induction simulated with an OGCM," *Ocean Sci. Discuss.*, vol. 12, no. 4, pp. 1869–1891, 2015.
[42] T. P. Boyer, "Linear trends in salinity for the world ocean, 1955–1998," *Geophys. Res. Lett.*, vol. 32, no. 1, pp. 67–106, 2005.
[43] F. M. Hamzah, O. Jaafar, S. R. M. Sabri, M. T. Ismail, K. Jaafar, and N. Arbin, "The interaction of physical properties of seawater via statistical approach," in *Proc. AIP Conf.*, 2015, vol. 1677, no. 1, Art. no. 110011, doi: 10.1063/1.4930782.
[44] R. Fuenzalida, W. Schneider, J. Garcés-Vargas, L. Bravo, and C. Lange, "Vertical and horizontal extension of the oxygen minimum zone in the eastern south pacific ocean," *Deep Sea Res. II, Topical Stud. Oceanogr.*, vol. 56, no. 16, pp. 992–1003, Jul. 2009.
[45] J. L. Reid, "On the temperature, salinity, and density differences between the atlantic and pacific oceans in the upper kilometre," *Deep Sea Res.*, vol. 7, no. 4, pp. 265–275, Mar. 1961.
[46] J. Zhang and M. Steele, "Effect of vertical mixing on the atlantic water layer circulation in the arctic ocean," *J. Geophys. Res.*, vol. 112, no. C4, pp. 854–871, 2007.
[47] S. Tabata, "Characteristics of water and variations of salinity, temperature, and dissolved oxygen content of the water at ocean weather station 'P' in the Northeast Pacific Ocean," *J. Fish. Res. Board Canada*, vol. 17, no. 3, pp. 353–370, 1960.
[48] V. W. Ekman, H. U. Sverdrup, M. W. Johnson, and R. H. Fleming, "The oceans, their physics, chemistry and general biology," *Geogr. Ann.*, vol. 27, pp. 388–391, 1945, doi: 10.2307/520072.
[49] G. Gao, M. Shi, J. Zhao, Z. Dong, G. Ji, and Y. Jiao, "Hydrologic features of the Bering Sea in the summer of 1999," *Acta Oceanol. Sinica*, vol. 24, no. 1, pp. 8–16, 2002.
[50] R. Pawlowicz, "A model for predicting changes in the electrical conductivity, practical salinity, and absolute salinity of seawater due to variations in relative chemical composition," *Ocean Sci.*, vol. 6, no. 1, pp. 361–378, 2010.
[51] R. Pawlowicz, "Calculating the conductivity of natural waters," *Limnology Oceanogr., Methods*, vol. 6, no. 9, pp. 489–501, Sep. 2008.
[52] R. B. McCleskey, "Electrical conductivity of electrolytes found in natural waters from (5 to 90) °C," *J. Chem. Eng. Data*, vol. 56, no. 2, pp. 317–327, Feb. 2011.
[53] A. B. Gancy and S. B. Brummer, "Conductance of aqueous electrolyte solutions at high pressures. Data for eleven 1,1 electrolyte systems," *J. Chem. Eng. Data*, vol. 16, no. 4, pp. 385–388, Oct. 1971.
[54] P. Wang and A. Anderko, "Modeling thermal conductivity of electrolyte mixtures in wide temperature and pressure ranges: Seawater and its main components," *Int. J. Thermophys.*, vol. 33, no. 2, pp. 235–258, Feb. 2012.
[55] T. Dauphinee, J. Ancsin, H. Klein, and M. Phillips, "The electrical conductivity of weight diluted and concentrated standard seawater as a function of salinity and temperature," *IEEE J. Ocean. Eng.*, vol. 5, no. 1, pp. 28–41, 2003.
[56] V. S. Bukhman, V. M. Timets, N. E. Shvede, and V. V. Lyachnev, "Metrological support for measurements of the electrical conductivity of seawater," *Meas. Techn.*, vol. 34, no. 4, pp. 389–391, Apr. 1991.

[57] T. J. McDougall, D. R. Jackett, and F. J. Millero, "An algorithm for estimating absolute salinity in the global ocean," *Ocean Sci. Discuss.*, vol. 6, no. 1, pp. 215–242, 2009.
[58] Z. Zheng, Y. Fu, K. Liu, R. Xiao, X. Wang, and H. Shi, "Three-stage vertical distribution of seawater conductivity," *Sci. Rep.*, vol. 8, no. 1, Dec. 2018, Art. no. 9916.
[59] H. A. Dijkstra, *Nonlinear Physical Oceanography: A Dynamical Systems Approach to the Large Scale Ocean Circulationand El Niño*, vol. 28. Springer, 2005.
[60] H. Renssen, H. Goosse, and T. Fichefet, "On the non-linear response of the ocean thermohaline circulation to global deforestation," *Geophys. Res. Lett.*, vol. 30, no. 2, pp. 31–33, Jan. 2003.
[61] R. A. F. Bilbao, J. M. Gregory, N. Bouttes, M. D. Palmer, and P. Stott, "Attribution of ocean temperature change to anthropogenic and natural forcings using the temporal, vertical and geographical structure," *Climate Dyn.*, vol. 53, nos. 9–10, pp. 5389–5413, Nov. 2019.
[62] O. Gottlieb and S. C. S. Yim, "Nonlinear oscillations, bifurcations and chaos in a multi-point mooring system with a geometric nonlinearity," *Appl. Ocean Res.*, vol. 14, no. 4, pp. 241–257, Jan. 1992.
[63] H. Hussmann, "Thermal equilibrium states of Europa's ice shell: Implications for internal ocean thickness and surface heat flow," *Icarus*, vol. 156, no. 1, pp. 143–151, Mar. 2002.
[64] J. A. Carton, S. A. Grodsky, and H. Liu, "Variability of the oceanic mixed layer, 1960–2004," *J. Climate*, vol. 21, no. 5, pp. 1029–1047, 2010.
[65] W. D. Gardner, S. P. Chung, M. J. Richardson, and I. D. Walsh, "The oceanic mixed-layer pump," *Deep Sea Res. II Top. Stud. Oceanogr.*, vol. 42, no. 2, pp. 757–775, 1995.
[66] R. R. Rao and R. Sivakumar, "Seasonal variability of sea surface salinity and salt budget of the mixed layer of the north Indian Ocean," *J. Geophys. Res.*, vol. 108, no. C1, pp. 1–9, 2003.
[67] M. G. Keerthi, M. Lengaigne, J. Vialard, C. de Boyer Montégut, and P. M. Muraleedharan, "Interannual variability of the Tropical Indian Ocean mixed layer depth," *Climate Dyn.*, vol. 40, nos. 3–4, pp. 743–759, Feb. 2013.
[68] N. Kolodziejczyk, G. Reverdin, and A. Lazar, "Interannual variability of the mixed layer winter convection and spice injection in the eastern subtropical North Atlantic," *J. Phys. Oceanogr.*, vol. 45, no. 2, pp. 504–525, Feb. 2015.
[69] T. Toyoda *et al.*, "Interannual-decadal variability of wintertime mixed layer depths in the north pacific detected by an ensemble of ocean syntheses," *Climate Dyn.*, vol. 49, no. 3, pp. 891–907, Aug. 2017.
[70] S. Gao, M. Zhou, Y. Wang, J. Cheng, H. Yachi, and J. Wang, "Dendritic neuron model with effective learning algorithms for classification, approximation and prediction," *IEEE Trans. Neural Netw. Learn. Syst.*, vol. 30, no. 2, pp. 601–614, Feb. 2019.

**YANG FU** received the B.S. degree from the Nanjing University of Information Science and Technology, Nanjing, China, in 2012, and the M.S. degree from Beijing Normal University, Beijing, China, in 2015. She is currently a Research Associate with the Shenyang Institute of Automation, Chinese Academy of Sciences, Shenyang, China. Her research interests are in data mining, time series analysis, data modeling, and sentiment analysis.

**ZEYU ZHENG** received the B.S. degree in mechanical engineering from Zhejiang University, Zhejiang, China, in 1997, and the Ph.D. degree from The Graduate University for Advanced Studies, Japan, in 2005. He is currently a Professor with the Institute of Automation, Chinese Academy of Sciences, Shenyang, China. He has authored nearly 50 technical articles in journals and conference proceedings. His research interests are in intelligent optimization algorithms, big data processing technology, data mining, project management, and complex systems.

**MENGCHU ZHOU** (Fellow, IEEE) received the B.S. degree in control engineering from the Nanjing University of Science and Technology, Nanjing, China, in 1983, the M.S. degree in automatic control from the Beijing Institute of Technology, Beijing, China, in 1986, and the Ph.D. degree in computer and systems engineering from the Rensselaer Polytechnic Institute, Troy, NY, USA, in 1990. He joined the New Jersey Institute of Technology (NJIT), Newark, NJ, USA, in 1990, where he is currently a Distinguished Professor of electrical and computer engineering. He has over 800 publications, including 12 books, over 500 journal articles (over 400 in IEEE transactions) and 29 book-chapters. He holds 23 patents. His research interests are in Petri nets, intelligent automation, the Internet of Things, big data, web services, and intelligent transportation. He is a Fellow of the International Federation of Automatic Control (IFAC), the American Association for the Advancement of Science (AAAS), and the Chinese Association of Automation (CAA). He is a Life Member of the Chinese Association for Science and Technology-USA and served as its President, in 1999. He was a recipient of the Humboldt Research Award for U.S. Senior Scientists from the Alexander von Humboldt Foundation, the Franklin V. Taylor Memorial Award, and the Norbert Wiener Award from the IEEE Systems, Man and Cybernetics Society. He is the Founding Editor of the *IEEE Press Book Series on Systems Science and Engineering* and the Editor-in-Chief of the IEEE/CAA JOURNAL OF AUTOMATICA SINICA.

**HAITAO YUAN** (Member, IEEE) received the B.S. and M.S. degrees in software engineering from Northeastern University, Shenyang, China, in 2010 and 2012, respectively, and the Ph.D. degree in control science and engineering from Beihang University, Beijing, China, in 2016. From 2013 to 2014, he was a Ph.D. student with the Department of Computer Science, City University of Hong Kong, Hong Kong. He was also a Visiting Doctoral Student with NJIT, in 2015. He has over 50 publications in international journals and conference proceedings, including IEEE TRANSACTIONS ON AUTOMATION SCIENCE AND ENGINEERING, the IEEE TRANSACTIONS ON SERVICES COMPUTING, the IEEE TRANSACTIONS ON INDUSTRIAL INFORMATICS, the IEEE TRANSACTIONS ON CYBERNETICS. His research interests include cloud computing, data center, big data, machine learning, optimization algorithms, and software-defined networking. He was the recipient of the 2011 Google Excellence Scholarship, and the recipient of the Best Paper Award-Finalist in the 16th IEEE International Conference on Networking, Sensing and Control.

**XIWANG GUO** received the B.S. degree in computer science and technology from the Shenyang Institute of Engineering, Shenyang, China, in 2006, the M.S. degree in aeronautics and astronautics manufacturing engineering. from Shenyang Aerospace University, Shenyang, in 2009, and the Ph.D. degree in system engineering from Northeastern University, Shenyang, in 2015. From 2016 to 2018, he was a Visiting Scholar with the Department of Electrical and Computer Engineering, New Jersey Institute of Technology, Newark, NJ, USA. He is currently an Associate Professor with the College of Computer and Communication Engineering, Liaoning Shihua University. He has authored over 30 technical articles in journals and conference proceedings, including the IEEE TRANSACTIONS ON CYBERNETICS, the IEEE TRANSACTIONS ON SYSTEM, MAN AND CYBERNETICS: SYSTEMS, the IEEE TRANSACTIONS ON INTELLIGENT TRANSPORTATION SYSTEMS, and the IEEE/CAA JOURNAL OF AUTOMATICA SINICA. His current research interests include Petri nets, remanufacturing, recycling and reuse of automotive, and intelligent optimization algorithm.